97-103

Environment Canada

Water Science and Technology Directorate

Direction générale des sciences et de la technologie, eau

Environnement Canada

In-Situ remediation of chromate contaminated groundwater using permeable reactive walls

By:
D. Blowes, C. Ptacek, J. Jambor

TD
226
N87
No. 97-
103

97-103

MANAGEMENT PERSPECTIVE

Title: In-situ remediation of chromate contaminated groundwater using permeable reactive walls.

Author: D.W. Blowes, **C.J. Ptacek**, and J.L. Jambor

NWRI Publication#: 97-103

Citation: Environmental Science and Technology

EC Priority/Issue: This study supports the ESD issue Conserving Canada's Ecosystems (metals). It supports the business plan deliverable Thurst #3 for toxics (groundwater remediation), and the EC Action Plan "Conserving Canada's Ecosystems" with the focus "Develop and implement strategies to conserv ecosystems". The study was initiated in 1991 and was funded by the University of Waterloo and the Natural Science and Engineering Research Council.

Current Status: The paper describes the results of batch tests, long-term column studies and mineralogical analyses conducted to assess the potential for in-situ reactive walls to remediate chromate contaminated groundwater. Chromium in the form of chromate is one of the most frequently encountered contaminants in groundwater. In the hexavalent form, Cr is highly toxic and carcinogenic. The study was initiated in 1992 and results of experiments conducted to assess the long-term potential of reactive walls for continued treatment of Cr(VI) are presented.

Next Steps: In-situ remediation appears to be a viable technique for remediation of a number of inorganic contaminants. Future efforts will be directed toward the development of techniques for remediating a variety of inorganic contaminants.

Abstract

Permeable-reactive redox walls, placed below the ground surface in the path of flowing groundwater, provide an alternative remediation approach for removing electroactive chemicals from contaminated groundwater. Geochemical calculations suggest that reduction of CrO_4^{2-} by reduced Fe (Fe^0 or Fe^{2+}) is thermodynamically favored under a range of geochemical conditions. Four types of Fe-bearing solids, siderite ($FeCO_3$), pyrite (FeS_2), coarse-grained elemental iron (Fe^0), and fine-grained Fe^0, were assessed for their ability to remove dissolved CrO_4^{2-} from solution at flow rates typical of those encountered at sites of remediation. Time-to-equilibrium batch studies show that the rate of CrO_4^{2-} removal by fine-grained Fe^0 is greater than that for pyrite and coarse-grained Fe^0, and that the rate of removal for pyrite and coarse-grained Fe^0 is dependent on pH. The rate of CrO_4^{2-} removal by reaction with fine-grained Fe^0, as indicated by these time-to-equilibrium studies, is much greater than would be required for treatment at rapid groundwater flow rates. Results from flow-through column studies suggest that partial removal of CrO_4^{2-} by pyrite and coarse-grained Fe^0 and quantitative removal of CrO_4^{2-} by fine-grained Fe^0 occurs at rapid groundwater flow velocities. The removal mechanism for CrO_4^{2-} by fine-grained Fe^0 and coarse-grained Fe^0 is through the reduction of Cr(VI) to Cr(III) coupled with the oxidation of Fe^0 to Fe(II) and Fe(III), and the subsequent precipitation of a sparingly soluble mixed Fe(III)-Cr(III) (oxy)hydroxide phase. Mineralogical analysis of the reactive material used in the batch tests indicates that Cr is associated with goethite (αFeOOH). These results suggest that Cr(III) is removed either through the formation of a solid-solution, or by adsorption of Cr(III) onto the goethite surface. The effective removal of Cr(VI) by Fe^0 under dynamic flow conditions suggests porous-reactive walls containing Fe^0 may be a viable alternative for treating groundwater contaminated by Cr(VI). There is also potential for treatment of other electrovalent metals using a similar approach.

In-Situ Remediation of Chromate Contaminated Groundwater Using Permeable Reactive Walls

David W. Blowes[a], Carol J. Ptacek[b,a], and John L. Jambor[a]

[a]Department of Earth Sciences, University of Waterloo, Waterloo, Ontario, Canada, N2L 3G1, e-mail: blowes@sciborg.uwaterloo.ca

[b]National Water Research Institute, Environment Canada, 867 Lakeshore Road, Burlington, Ontario, Canada, L7R 4A6

Abstract

Permeable-reactive redox walls, placed below the ground surface in the path of flowing groundwater, provide an alternative remediation approach for removing electroactive chemicals from contaminated groundwater. Geochemical calculations suggest that reduction of CrO_4^{2-} by reduced Fe (Fe^0 or Fe^{2+}) is thermodynamically favored under a range of geochemical conditions. Four types of Fe-bearing solids, siderite ($FeCO_3$), pyrite (FeS_2), coarse-grained elemental iron (Fe^0), and fine-grained Fe^0, were assessed for their ability to remove dissolved CrO_4^{2-} from solution at flow rates typical of those encountered at sites of remediation. Time-to-equilibrium batch studies show that the rate of CrO_4^{2-} removal by fine-grained Fe^0 is greater than that for pyrite and coarse-grained Fe^0, and that the rate of removal for pyrite and coarse-grained Fe^0 is dependent on pH. The rate of CrO_4^{2-} removal by reaction with fine-grained Fe^0, as indicated by these time-to-equilibrium studies, is much greater than would be required for treatment at rapid groundwater flow rates. Results from flow-through column studies suggest that partial removal of CrO_4^{2-} by pyrite and coarse-grained Fe^0 and quantitative removal of CrO_4^{2-} by fine-grained Fe^0 occurs at rapid groundwater flow velocities. The removal mechanism for CrO_4^{2-} by fine-grained Fe^0 and coarse-grained Fe^0 is through the reduction of Cr(VI) to Cr(III) coupled with the oxidation of Fe^0 to Fe(II) and Fe(III), and the subsequent precipitation of a sparingly soluble mixed Fe(III)-Cr(III) (oxy)hydroxide phase. Mineralogical analysis of the reactive material used

in the batch tests indicates that Cr is associated with goethite (αFeOOH). These results suggest that Cr(III) is removed either through the formation of a solid-solution, or by adsorption of Cr(III) onto the goethite surface. The effective removal of Cr(VI) by Fe^0 under dynamic flow conditions suggests porous-reactive walls containing Fe^0 may be a viable alternative for treating groundwater contaminated by Cr(VI). There is also potential for treatment of other electrovalent metals using a similar approach.

Keywords: Groundwater, chromium, elemental iron, remediation, reactive walls

Introduction

Conventional treatment programs for groundwater contaminated by redox-sensitive inorganic species, such as chromium, iron, sulfate, molybdenum, uranium, technetium, selenium and arsenic, have involved pumping groundwater to the land surface followed by treatment and redisposal. Pump-and-treat groundwater remediation methods have proven to be expensive and possibly ineffective *(1, 2)*. An alternative to pump-and-treat groundwater remediation is the use of porous, permeable, geochemically-reactive barriers *(3)*. These permeable barriers are installed in the path of flowing groundwater, either as horizontal treatment layers *(4 - 7)* or as vertical treatment walls *(8 - 18)*. These geochemical barriers are engineered through the addition of reactive solids. The contaminant is removed through *in situ* transformations, which results in its destruction or immobilization. For many dissolved metals treatment can be attained by enhancing reduction or oxidation of a chemical species, resulting in the precipitation of a sparingly-soluble solid *(11, 12)*. The results of laboratory experiments illustrate the potential for remediation of groundwater contaminated by hexavalent chromium. Hexavalent chromium was chosen as an

example, to demonstrate the potential application of permeable-reactive walls for treating groundwater contaminated by redox-sensitive inorganic species.

Permeable walls containing treatment mixtures can be installed in the path of flowing groundwater to passively remove dissolved constituents through a series of reactions. These reactive walls can be installed as either continuous treatment zones *(11)*, or they can be installed as impermeable barriers containing permeable zones or windows *(8, 19)*. Using excavation techniques, aquifer material is removed and replaced with the reaction mixtures. In place, groundwater moves through the treatment walls by natural flow processes, or, when necessary, pumping wells can be installed to direct contaminated water through the reactive materials (Fig. 1). To be effective as a reactive wall component the solid phase must be both sufficiently reactive to result in the desired chemical change and sufficiently insoluble to remain in place for an economically reasonable length of time.

Reduction of Cr(VI) to Cr(III) by Fe(II) occurs rapidly under acidic conditions *(20 - 23)*. Removal of Cr(VI) from wastewater, by initially reducing Cr(VI) to Cr(III) using dissolved Fe(II) and adding base to favor precipitation of insoluble Cr(III) precipitates, is a common practice *(20)*:

$$Cr(VI)(aq) + 3Fe(II)(aq) \rightarrow Cr(III)(aq) + 3Fe(III)(aq) \qquad (1)$$

This reaction is written for total Cr(VI), Cr(III), Fe(II) and Fe(III), in general, and not in terms of individual hydrolysis products such as $HCrO_4^-$, CrO_4^{2-}, $Cr(OH)_3^0$, and $Fe(OH)_3^0$, etc., to focus on the overall reaction process. Reaction one can be facilitated through the use of a number of Fe(II) sources, both Fe(II)-containing solutions and Fe(II)-containing solids. Examples of aqueous solutions include $FeSO_4$ or $FeCl_2$ solutions. Examples of solid-phase reductants include elemental iron, biotite, hematite, pyrite, magnetite, and other Fe(II)-bearing minerals *(11, 24 - 30)*. The most

rapid reduction, within minutes, occurs with Fe(II) added as a dissolved species *(20)*, although reduction rates using Fe-bearing solids can also proceed within tens of minutes *(20)*.

Whereas the rate of reduction is important, of greater interest for applications in porous wall settings, is the rate of removal of Cr(III) through precipitation of a sparingly soluble solid. This second step is often the rate limiting step for removal of Cr(III) from solution *(26)*. Under moderate pH conditions, removal of Cr(III) can occur through the precipitation of $Cr(OH)_3$:

$$Cr^{3+} + 3OH^- \rightarrow Cr(OH)_3(s) \qquad (2)$$

or through precipitation of mixed Fe(III)-Cr(III) hydroxide solid *(20)*

$$xCr(III) + (1-x)Fe(III) + 3H_2O \rightleftharpoons (Cr_xFe_{1-x})(OH)_3(s) + 3H^+ \qquad (3)$$

or mixed Fe(III)-Cr(III) (oxy)hydroxide solid *(31)*

$$xCr^{3+} + (1-x)Fe^{3+} + 2H_2O \rightleftharpoons Cr_xFe_{1-x}OOH_{(s)} + 3H^+ \qquad (4)$$

Analysis of a mixed Fe(III)-Cr(III) solid precipitated fresh from aqueous solution yielded a stoichiometry of $Cr_{0.25}Fe_{0.75}(OH)_3$ *(20)*. Following reaction (3), Eary and Rai concluded that at pH values between five and 11, precipitation of a mixed Cr(III)-Fe(III) hydroxide phase will generally limit total dissolved concentrations of Cr(III) to values less than the drinking water standard of 10^{-6} M.

Blowes and Ptacek *(11)* and Powell et al. *(30)* described batch experiments intended to

assess the potential for the removal of Cr(VI) in porous reactive walls. Powell et al. provided a detailed description of the effects of augmenting the reactive mixture with natural aquifer solids and proposed a reaction pathway to account for the catalytic effect of the aquifer solids. The present study assesses the ability of different solid-phase materials at removing dissolved Cr(VI) from synthetic groundwater under dynamic flow conditions over a sustained period of time. A particular focus of the study is on the effectiveness of different materials at removing Cr(VI) under the intermediate-pH conditions that typically would be found in a reactive wall setting. Geochemical calculations and time-to-equilibrium batch tests were conducted to pre-screen potential candidates for further study using dynamic flow-through column tests. The tests were conducted using three types of solids, siderite ($FeCO_3$), pyrite (FeS_2), and elemental iron (Fe^0). Two forms of Fe^0, coarse-grained chips and fine-grained filings, were evaluated. The experiments presented here were carried out to assess whether the rates of reaction were sufficiently rapid under dynamic flow conditions, whether the precipitates formed would occur as coatings that would potentially inhibit the reaction progress, and whether clogging of the porous media would occur preventing passage of the contaminated groundwater through the reactive material.

Experimental

A series of time-to-equilibrium batch experiments was conducted by adding 500 g of Cr-bearing solution (Cr(VI) added as K_2CrO_4 to $CaCO_3$ saturated double-deionized water, 25 mg/L as Cr in mixtures A and B, and 18 mg/L as Cr in mixtures C and D) to 100 g of solid mixture (Table 1). The elemental iron was obtained commercially as high-purity filings (~ 0.5 - 1 mm in diameter) and chips (~ 1 - 5 mm in diameter). The pyrite and calcite were natural materials

that were finely crushed (~ 0.5 - 2 mm in diameter). The quartz was washed Ottawa quartz sand (30 < mesh < 25). The mixtures were agitated at room temperature and intermittently sampled by allowing the solids to settle for 5 *min* then removing, by syringe, 10 mL of solution. The samples were filtered immediately through a 0.2 μm filter and acidified to pH < 1.0 for Cr analysis.

For the dynamic column experiments, six 6.5 cm diameter acrylic columns, five 15 cm in length and one 20 cm in length (Figure 2), were packed with the reactive mixtures using the solids according to Table 2. A multi-channel high-precision peristaltic pump was used to pass tracer solution through the columns, from their base upward, at a constant rate. Before introducing the Cr-bearing solution, solution containing Cl (prepared in a calcium-carbonate buffered solution as used for the batch experiments) was pumped through the columns to obtain information on the void volume and dispersivity of the column packing. The Cl solution was then flushed from the column with background solution (calcium-carbonate buffered solution), after which the Cr-bearing solution was input into the column. The Cr solution was prepared using the same method used in the batch tests. Input Cr(VI) concentrations of 80 mg/L were used for the control column experiment and the experiment containing siderite. Input cocentrations of 18 mg/L Cr(VI) were used for the experiments containing pyrite and Fe^0. Samples were collected at intervals of up to 1.5 *hr* using automatic fraction collectors during the first several weeks of the experiments. At later times the samples were collected manually. The pore water pH and Eh were determined using combination electrodes in sealed flow through cells. The pH was determined using a combination pH electrode (ORION Ross 815600). The pH electrode was calibrated using pH 4, pH 7 and pH 9.18 standard buffers (NBS standard). The response of the electrode was

confirmed before and after each reading. The response of the Eh electrode (ORION 96-7800) was confirmed with Zobell's solution *(32, 33)* and Light's solution *(34)*.

Samples for Cr analysis were collected directly in sufficient acid to lower the pH < 1.0. Concentrations of Cl were determined colorimetrically using the ferricyanide spectrophotometric method *(35)*, concentrations of Cr(VI) were determined colorimetrically using the diphenylcarbazide spectrophotometric method *(35)*, and concentrations of total Cr were determined by flame-emission atomic absorption spectroscopy. Additional samples were also periodically collected and analyzed for Ca, Cr, Cu, Fe, K, Mg, Mn, Na, and Zn by inductively coupled plasma emission spectroscopy (ICP) and for Cl and SO_4 by ion chromatography.

The composition of the stock iron filings was determined by Activation Laboratories Ltd. (Ancaster, Ontario). The concentrations of As, Ba, Cu, Mo, Ni, and Sb were determined by inductively coupled argon plasma atomic emission spectrometry (ICP-AES) following digestion.

The nature of the reaction product from the batch experiments, conducted using Fe^0 was characterized mineralogically. The reaction products were examined using reflected-light and scanning electron microscopy with X-ray dispersion analysis. The reaction products were also characterized by electron microbeam and Debye Scherer X-ray analyses.

Results and Discussion

Batch Experiments. Results of time-to-equilibrium studies indicate the rate of removal of Cr from solution varies substantially for the different mixtures assessed (Fig. 3). Removal of Cr from solution was most rapid for the mixture containing iron filings, intermediate for pyrite and least rapid for the coarse-grained iron chips. The rate of removal was also observed to vary with the

presence or absence of calcite. These results suggest that all of these materials may be suitable to remove Cr at low velocities and that iron filings should be the most suitable candidate material for use in porous redox walls in locations of rapid groundwater flow.

In contact with pyrite, in the presence of calcite, 50% of the Cr was removed after 6.5 *hrs*, with removal to < 0.05 mg/L within 20 *hrs*. In the absence of calcite removal was more rapid, with 50% removal observed within 1 *hr*., with removal to < 0.05 mg/L within 4 *hrs*. The pH of the supernatant solution was estimated using pH indicator strips throughout the experiment. These measurements indicate that the pH was similar whether calcite was present or absent, varying between 4.5 and 5.5.

In contact with iron chips, with and without calcite, 50% of the Cr was removed within 28 *hrs*. Within 50 *hrs* the supernatant concentration was < 0.05 mg/L. The pH of the supernatant solution, in both experiments, varied between 5.2 and 5.5. In contact with iron filings with calcite present, 50 % of the Cr was removed in < 2 *hrs*; 50 % of the Cr also was removed in < 2 *hrs* without calcite. In both cases the supernatant Cr concentration was < 0.05 mg/L within 3 *hrs* in contact with the iron filings. To assess the effect of varying temperature, batch experiments using iron filings were conducted at two temperatures 23±1°C and 4°C. These temperatures bracket conditions observed in many aquifers. The results show rapid Cr(VI) removal at both temperatures, with no discernable delay in Cr(VI) removal at the lower temperature. Rapid loss of Cr from solution in contact with Fe^0 is consistent with observations of previous studies *(27, 30)*. The pH of the supernatant solution varied from 4.9 to 5.5, lower than that indicated by Powell et al. *(30)*.

The initial iron filings and iron chips, and the reaction products of the experiments

conducted using iron filings and iron chips were characterized mineralogically. Portions of each sample were mounted in polished section for optical microscopic and microbeam examination. In addition, numerous loose fragments were examined by SEM. Several Debye-Scherrer X-ray patterns were obtained from loose material and the alteration phases contained in the polished sections.

Microprobe analysis of the iron chips indicates that, prior to reaction with the Cr(VI) solution, they are almost pure Fe (Table 3), whereas the iron filings contain small amounts of Si, Cr and P. The composition of the iron filings, prior to reaction with the Cr containing solution, was determined by digestion and subsequent analysis by ICP-AES. The results from this analysis indicate that the filings contain 92.2 mass % Fe, 5.2 mass % Si, 2.4 mass % Cr and small amounts of other elements.

The secondary phases identified were goethite, lepidocrocite, maghemite, and possibly hematite. No discrete chromium mineral was detected, but zones within the iron hydroxides contain up to 27.3 mass % $Cr(OH)_3$. The bulk of the iron hydroxide found was goethite. There are conspicuous local zones of maghemite layered with goethite. Lepidocrocite is the youngest phase and seems to be mainly at the surface of the oxyhydroxide layers. Hematite, unlike the other phases, was not detected in the Debye-Scherrer patterns, but a surface phase occurring as euhedral, hexagonal shaped plates is strongly suggestive of hematite on the basis of morphology and non-quantitative composition. The iron filings were air-dried, and stored and shipped in contact with the atmosphere prior to analysis. The formation of reaction products, notably lepidocrocite, maghemite, and hematite, may have occurred following reaction during the experiment, indicating the importance of goethite and less-ordered precursors in the removal of

Cr from solution.

Examination of the Fe chips and filings indicates that Cr is not associated with each pellet. In addition, the Cr-rich zones are not uniformly distributed within specific areas of the iron hydroxides. Some trends, however, can be seen in the SEM micrographs. Figure 4a illustrates the apparent randomness of the association between oxyhydroxides and Cr in that there are five different areas of oxyhydroxides within the chip, but only one is Cr-bearing. Enlargement of the Cr-bearing veinlet (Figure 4b), shows that the Cr-rich phase is concentrated at one end of the veinlet, and also among its margins. Microprobe analyses (Table 3) gave up to 20 wt% Cr_2O_3. The corresponding SEM X-ray maps of the veinlet show a strong correlation between Cr and Si, and this association is confirmed by the microprobe results.

Electron-microprobe Fe_2O_3 values (total Fe as Fe_2O_3; Table 3) for the oxyhydroxides in Figure 4b range from 57.5 to 99.8 wt%. The theoretical Fe_2O_3 contents of goethite are 89.86 wt%, and those of hematite are 100 wt%. Lepidocrocite has the same Fe_2O_3 content as goethite, and maghemite has the same content as hematite. As mentioned, the relative abundances of the phases suggest that we are dealing mainly with goethite and maghemite; thus, in Table 3 it can be inferred from the analytical totals that the maghemite contains little Cr.

Figure 5 shows the secondary phases in a vug in the iron. The X-ray maps again show a strong correlation between Cr and Si, but the microprobe analyses (Table 3) indicate that the correlation is coincidental rather than specific: the highest and second highest Cr values (20.2 and 19.9 wt% Cr_2O_3) are accompanied by the lowest (0.4%) and the highest (8.6%) SiO_2 values, respectively.

Coatings of iron oxyhydroxides occur on the iron filings, but the interior replacement of

the filings gives textures that are substantially different from those in the chips. This difference arises because the chips are homogeneous and massive, whereas the host iron of the filings is a grid-like intergrowth of the two principal phases. Figure 6 illustrates an iron oxyhydroxide coating that formed as an inter-grain cement. The accompanying X-ray map for Cr shows that this element is localized in only part of the oxyhydroxide mass; moreover, the highest Cr concentrations seem to occur where the convex margins of the oxyhydroxides meet. X-ray maps show the close association between Cr and Si, exactly as occurs with the secondary phases that accompany the iron chips. Electron microprobe analyses of the seven areas marked on Figure 6 are given in Table 4. Areas 5, 6, and 7 have compositions characteristic of maghemite, which is in accord with the X-ray data. Only a trace of Cr_2O_3 was detected in one analysis of the maghemite, which is in agreement with the previous results (Table 4) suggesting that Cr uptake by maghemite is low. The results for the analysis of the accompanying presumed goethite are similar to those given in Table 4.

Electron-microprobe analyses of the filings (Figure 7,8; Table 5) indicate that the whiter phase (as seen in SEM) contains 0.2-0.3 wt% Cr, about 0.1 wt% P, and about 1.9 wt% Si. The darker (matrix) phase contains about 0.9 wt% Cr, and variable Si and P (up to 0.6 wt% Si and 0.7% wt% P).

In summary, the secondary phases identified in the samples are lepidocrocite, maghemite, goethite, and probably hematite. The last is rare; lepidocrocite is sparse, and seems to be concentrated as a late-stage, surface phase (as is hematite). Maghemite is common, but is of minor abundance relative to that of goethite. All of the phases except goethite are characteristically low in Cr; whether Cr has been taken into solid solution in the goethite

structure is not known, but such substitution has been experimentally demonstrated *(31)*. The microprobe and SEM results also showed that there is a coincidental association of Cr and Si, and that high Si values in the secondary assemblage occur only in the presence of goethite. SiO_2 values in some instances exceed 10 wt%, well beyond the possibility of structural incorporation of Si. As no discrete Si phase was detected in the mineralogical study, the indication is that the Si occurs as an amorphous phase adsorbed on goethite. The possibility that Cr and Ca occur as adsorbed phases cannot be discounted, however, the mass ratios of Fe to Cr observed in the mineralogical study are similar to those previously observed by Eary and Rai *(20)*. This similarity suggests similar processes result in the incorporation of Cr into the Fe(III)-bearing phase in both cases.

The strong association of Cr and Si in the secondary phases is consistent with observations made by Powell et al. *(30)*, who observed a faster rate of reaction in the presence of aluminosilicates. Powell et al. *(30)* attribute this catalytic effect to aluminosilicate dissolution under high pH conditions, which moderates the pH.

Flow-through Column Experiments. To assess the effectiveness of these reactive mixtures under dynamic flow conditions, and to assess the mass of reactant required, flow-through column experiments were conducted using reactive mixtures containing 5 mass % siderite ($FeCO_3$), 20 mass % pyrite, 10 mass % iron chips, and 50 mass % iron filings (Table 2). A control experiment containing 100% quartz sand was conducted at a transport velocity of 25 m/a (column 1). A transport velocity of 20 m/a was used for the columns containing siderite (column 2) and pyrite (column 3), and 10 m/a was used for the column containing iron chips (column 4) and one column containing iron filings (column 5). A second column experiment containing iron filings

was also conducted at a higher velocity of 40 m/a (column 6).

Transport conditions within the columns were assessed using Cl^- as a conservative tracer (Figs. 9 - 14). The program CXTFIT *(36)*, a non-linear least squares algorithm, was applied to the experimental results to determine solute transport parameters for the one-dimensional advection dispersion equation from experimental data (Figs. 9-14). The analytical solution for constant flux boundary conditions and semi-infinite length was assumed and dispersion coefficients were obtained as fitted parameters. Predicted breakthrough curves calculated with the fitted dispersion coefficient are in close agreement with the experimental data, suggesting uniform flow conditions were present in the columns (Figs. 9 - 14).

In the control experiment containing 100% silica sand (column 1, Fig. 9), breakthrough of Cr(VI) was observed at one pore volume (total effluent volume/void space volume within the column), and coincided with the breakthrough of Cl. Cr(VI) concentrations increased from below detection (0.05 mg/L) to the input concentration within one pore volume.

In the column containing siderite (column 2, Fig. 10), high concentrations of Cr(VI) were present in the effluent water from the first pore volume onward. The upper plateau of the Cr(VI) breakthrough curve shows some variability that may arise from partial reduction of Cr(VI), or analytical error. Although the data suggest that some reduction may have occurred, the degree of removal is not sufficient for siderite to be considered a viable material for use in a reactive wall for Cr(VI) treatment. The siderite used was derived from a natural source that was hydrothermally emplaced. As a result of its high temperature of formation the crystallinity of the solid phase was also very high, limiting the available surface area for the reduction reaction. In addition, the siderite used may have contained significant concentrations of impurities, such as

Fe(III). The presence of these impurities may also have limited the rate of reaction at the mineral surface. No further tests were conducted using the column which contained siderite.

The column containing pyrite showed removal of Cr for 3.5 pore volumes (column 3, Fig. 11). After 3.5 pore volumes the Cr concentration increased to the influent concentration (18 mg/L) within one additional pore volume. Prior to breakthrough, treatment of Cr was irregular. No further tests were conducted on the column containing pyrite.

In the column containing iron chips (column 4, Fig. 12), Cr was absent from the effluent for 4.5 pore volumes. Brown alteration coatings, inferred to be ferric oxyhydroxide, were observed to form on the iron chips as the Cr-bearing solution flowed through the column. After 4.5 pore volumes the Cr concentration increased to the input concentration of 18 mg/L within one additional pore volume. The removal of Cr(VI) in the column containing iron chips was probably limited by both the mass of iron in the column and the available surface area. At the time of Cr(VI) breakthrough, however, significant mass of iron remained in the column, and the principal inhibition to Cr(VI) reduction was probably the available surface area, which declined as a result of ferric oxyhydroxide precipitation. The mineralogical analysis from the batch experiments indicated that the iron surface is coated with ferric iron oxyhydroxides, which would inhibit the rate of reduction.

Two column experiments were conducted using iron filings. These experiments varied in the flow rate of the influent solution. The first column experiment containing iron filings (column 5, Fig. 13) was conducted at a pore water velocity of 10 m/a, the same velocity used for the column containing iron chips. This velocity was selected to be representative of pore water velocities observed at known sites of groundwater contamination. Cr(VI) was absent (< 0.05

mg/L) from the effluent for more than 150 pore volumes, when the experiment was terminated. No evidence of Cr release from this column was observed. There was some evidence of ferric oxyhydroxide formation on the surfaces of the iron filings, particularly at the influent end of the column. Continual treatment of Cr(VI) was observed, suggesting that the filing surfaces remained reactive throughout the duration of the experiment.

The effluent water collected from column 5 was slightly basic ($9.25 < pH < 10$) and moderately reduced ($250\ mV < Eh < 450\ mV$). The dominant cations in the water were Ca and K, with lesser concentrations of Na (Table 6). Bicarbonate was the dominant anion, with lesser concentrations of Cl. The dissolved Cr concentration remained < 0.02 mg/L and the effluent Fe concentration was < 0.002 mg.L. Geochemical modelling was conducted using the geochemical-speciation/mass-transfer model MINTEQA2 *(37)*. In these simulations the concentrations of Fe and Cr which were below detection limit were assumed to be equal to the analytical detection limit for that element. The pH and Eh were fixed at the values measured in the laboratory. The results of the calculations for two water samples (Table 6) indicate that the effluent water is slightly supersaturated with respect to calcite [$CaCO_3$], ferrihydrite [$Fe(OH)_3$], and amorphous chromium hydroxide [$Cr(OH)_3$]. The effluent water is supersaturated with respect to goethite [FeOOH], and undersaturated with respect to siderite [$FeCO_3$] and amorphous SiO_2. These results are consistent with the mineralogical observations of the reaction products of the batch experiments, which indicate that goethite is the most abundant reaction product, and that Cr and SiO_2 are retained as coprecipitates within the goethite structure.

The second experiment using a column containing iron filings (column 6, Fig. 14) was conducted at an average linear velocity of 40 m/a, four times the velocity of the other column

experiment conducted with iron filings. This higher velocity was selected to hasten the breakthrough of Cr(VI). At this higher velocity Cr(VI) removal was observed for more than 80 pore volumes (Region I; Fig. 14). At 100 pore volumes the Cr(VI) concentration increased to more than 50% of the influent Cr(VI) concentration. Throughout the duration of the first portion of the experiment (Region I; Fig. 14), upward migration of a front of ferric oxyhydroxide precipitates was observed. Breakthrough of Cr(VI) in the column effluent coincided with arrival of the ferric oxyhydroxide front at the effluent end of the column.

At 137 pore volumes the influent solution was switched from the Cr(VI) bearing solution to a Cr-free calcium carbonate saturated solution to assess the extent of Cr leaching from the Cr-bearing precipitates contained in the column. Cr concentrations in the effluent declined within two pore volumes to the analytical detection of 0.05 mg/L and remained below detection for the subsequent 350 pore volumes (Region II; Fig. 14). Flushing the column with the Cr-free solution was accompanied by a gradual disappearance of the visible ferric oxyhydroxides. This disappearance is attributed to the reduction of Fe(III) by Fe^0 through reaction of the form:

$$2Fe^{3+} + Fe^0 \rightleftharpoons 3Fe^{2+}$$

The concentrations of Cr and Fe(II) were monitored throughout the leaching stage of the experiment (Region II; Fig. 14). Throughout this period the Cr(VI) and the Cr_{total} concentrations remained below the analytical detection limit. The Fe(II) concentration remained low, generally less than 1 mg/L. These concentrations of Fe(II) are too low to represent an environmental concern in a field setting.

Approximately 150 pore volumes after the initiation of flushing with the Cr-free input solution, most of the visible ferric oxyhydroxides were removed. At 514 pore volumes, the input

solution containing Cr(VI) was recommenced (Region III; Fig. 14), and the effluent Cr concentration was monitored. Removal of Cr to below the analytical detection limit was observed for an additional 98 pore volumes; a treatment period of about the same duration as the initial period of treatment. These preliminary results suggest that it may be possible to regenerate the reactive material in the porous wall, *in situ*, by flushing the wall with clean water or a mild reductant. Such a treatment would probably be less expensive than the reinstallation of the entire reactive wall, and would extend the life-span of an individual installation.

The columns with iron filings contained a greater mass of iron (50 wt% Fe) than the one with iron chips (10 wt. %) (Table 2), and the surface area of the iron filings is greater than that of the iron chips. These two factors probably contributed to the greater reactivity, and improved treatment in the column containing the iron filings. In addition, of the two column experiments conducted using iron filings, the lower velocity experiment (10 m/a *versus* 40 m/a) show superior treatment. This observation is consistent with a hypothesis that suggests that the extent of treatment is dependent on the degree of contact between the dissolved Cr(VI) and the Fe^0 surface. Under lower velocity conditions, transport to the reactive iron surfaces would be enhanced by the increased time available for diffusion through alteration coatings on the iron filing surface. Consideration of the potential benefits of increased residence times within the reactive zone in the porous barrier should be considered in the design of the *in situ* treatment system.

Conclusions

Porous redox walls are an alternative to conventional pump-and-treat remediation schemes for

groundwater contaminated with electroactive species. Laboratory time-to-equilibrium batch experiments and flow-through column experiments demonstrate that hexavalent chromium can be reduced and removed from solution in porous reactive walls at rapid groundwater flow rates. Of the potential reactive materials tested, iron filings showed greater reactivity than iron chips, pyrite, or siderite. The column experiments conducted using iron filings showed removal of Cr, to below analytical detection limits for up to 150 pore volumes. No Cr was detected in the column effluent during flushing by more than 150 pore volume of a Cr-free input solution, after breakthrough of Cr(VI), suggesting that the precipitate formed will retain the precipitated Cr after treatment is complete. Flushing with the Cr-free input water regenerated the reactivity of the Cr column, suggesting that flushing with water or a mild reducing solution may provide a simple and inexpensive method to regenerate the reactivity of a porous wall *in situ*. Experiments are underway to assess the applicability of this approach to the treatment of groundwater contaminated by other electroactive chemicals.

Acknowledgements

C.J. Hanton-Fong assisted with the experimental study and with the interpretation of the column effluent data, her assistance is gratefully acknowledged. K. Zhou, K. Madsen and S. Dyrkton and K. DeVos assisted with the batch and column experiments. Funding for this research was provided by the Natural Sciences and Engineering Research Council of Canada, through a grant provided to the first author.

Literature Cited

(1) Mackay, D.M.; Cherry, J.A. *Environ. Sci. Technol.*, **1989**, 23, 630-636.

(2) Mackay, D.M.; Feenstra, S.; Cherry, J.A. In Neretnieks, I., Ed., Proc. Workshop Contaminated Soils - Risks and Remedies, Stockholm, Oct. 6-28, 1993, pp. 35-47.

(3) Blowes, D.W.; Ptacek, C.J.; Cherry, J.A.; Gillham, R.W.; Robertson, W.D. Proc. 1995 Am. Soc. Civil Eng. Conf. and Exhibition, *The Geoenvironment 2000*, New Orleans, LA, February 24-26, in press.

(4) Artiole, J.; Fuller, W.H. *J. Environ. Qual.*, **1979**, 8, 503-510.

(5) Longmire., P.A.; Brookins, D.G.; Thomson, B.M.; Eller, P.G. Mat. Res. Soc. Symp. Proc., **1991**, 212, 623-631.

(6) Morrison, S.J.; Spangler, R.R. *Environ. Sci. Technol.*, **1992**, 26, 1922-1931.

(7) Morrison, S.J.; Spangler, R.R. *Environ. Prog.*, **1993**, 12, 175-181.

(8) McMurty, L.J.; Elton, R.O. *Environ. Prog.*, **1985**, 4, 168-170.

(9) Thomson, B.M.; Shelton, S.P. Proceedings of Focus Conference on Southwestern Ground Water Issues, March 23-25, 1988, Albuquerque, New Mexico, pp. 44-453.

(10) Thomson, B.M.; Shelton, S.P.; Smith, E. 45th Purdue Industrial Waste Conference Proceedings, Lewis Publishers, 1992, pp. 73-80.

(11) Blowes, D.W.; Ptacek, C.J. Proc. Subsurface Restoration Conf., 3rd International Conf. on Ground Water Quality Res., June 21-24, 1992, Dallas, Texas, pp. 214-216.

(12) Blowes, D.W.; Ptacek, C.J. *United States Patent* 5,362,394, 1994.

(13) Gillham, R.W.; O'Hannesin, S.F. IAH Conf. *Modern Trends in Hydrogeology*, Hamilton, Ontario, May 10-13, 1992., pp. 94-103.

(14) Gillham, R.W.; O'Hannesin, S.F. *Ground Water*, **1994**, 32, 958-967.

(15) Bianchi-Mosquera, G.C.; Allen-King, R.M.; Mackay, D.M. *Groundwater Mont. Remediation*, **1994**, 120-128.

(16) Ptacek, C.J.; Blowes, D.W.; Robertson, W.D.; Baker, M.J. Proc. Waterloo Centre for Groundwater Research Annual Septic System Conference, Wastewater Nutrient Removal Technologies and Onsite Management Districts, Waterloo, Ontario, June 6, 1994, pp. 26-44.

(17) Robertson, W.D.; Cherry, J.A. *Ground Water*, in press.

(18) Blowes, D.W.; Ptacek, C.J.; Bain, J.G.; Waybrant, K.R.; Robertson, W.D. Proc. Sudbury '95 Conference, Mining and the Environment, Sudbury, Ontario, May 28-June 1, 1995, in press.

(19) Starr, R.C.; Cherry, J.A. *Ground Water*, **1994**, 32, 465-476.

(20) Eary, L.E.; Rai, D. *Environ. Sci. Technol.*, **1988**, 22, 972-977.

(21) Saleh, F.Y.; Parkerton, T.F.; Lewis, R.V.; Huang, J.H.; Dickson., K.L. *Sci. Total Environ.*, **1989**, 86, 25-41.

(22) Palmer, C.D.; Wittbrodt, P.R. *Environ. Health Perspect.*, **1991**, 92, 25-40.

(23) Nriagu, J.; Beaubien, S.; Blowes, D.W. *Environ. Rev.*, **1993**, 1, 104-120.

(24) Gould, J.P. *Water Res.*, **1982**, 16, 871-877.

(25) Bowers, A.R.; Ortiz, C.A.; Cardoza, R.J. 1986. *Metal Finishing*, **1986**, 84, 37-??

(26) Eary, L.E.; Rai, D. *Am. J. Sci.*, **1989**, 289, 180-213.

(27) Bostick, W.D.; Shoemaker, J.L.; Osborne, P.E.; Evans-Brown, B. In: Tedder, D.W.; Pohland, F.G., Eds., *Emerging Technologies in Hazardous Waste Management*, Am.

Chem. Soc. Symp. Ser. 422, 1990, pp. 345-367.

(28) Anderson, L.D.; Kent, D.B.; Davis, J.A. *Environ. Sci. Technol.*, **1994**, 28, 178-185.

(29) Kent, D.B.; Davis, J.A.; Anderson, L.C.D.; Rea, B.A.; Waite, T.D. *Water Resour. Res.*, **1994**, 30, 1099-1114.

(30) Powell, R.M; Puls, R.W.; Hightower, S.K.; Sabantini, D.A. *Environ. Sci. Technol.*, **1995**, 29, 1913-1922.

(31) Schwertmann, U.; Gasser, U.; Sticher, H. *Geochim. Cosmochim. Acta*, **1989**, 53, 1293-1297.

(32) ZoBell, C.E. *Bull. Am. Assoc. Petrol. Geol.*, **1946**, 30, 477-509.

(33) Nordstrom, D.K. *Geochim. Cosmochim. Acta*, **1977**, 41, 1835-1841.

(34) Light, T.S. *Anal. Chem.*, **1972**, 44, 1038-1039.

(35) Standard Methods for the Examination of Water and Wastewater, 18th Edition. In: Greenberg, A.E.; Cleceri, L.S.; Eaton, A.D. (Eds.), American Health Association, Washington, D.C., 1992.

(36) Parker, J.C.; van Genuchten, M.Th. 1984. Virginia Agriculture Experimental Station Bull. 84-3, 1984, 96 pp.

(37) Allison J.D.; Brown, D.S.; Novo-Gradac, K.J. MINTEQA2/PRODEFA2, A Geochemical Assessment Model for Environmental Systems: Version 3.0 User's Manual. U.S. Environ. Prot. Agency, GA, **1990**, 106 pp.

Table 1. Composition of mixtures used in time-to-equilibrium batch experiments.

Sample	Reactive Mixture Compositions (mass %)				
	Iron Filings	Iron Chips	Pyrite	Calcite	Quartz Sand
A-1	50.	-	-	1.	49.
A-2	50.	-	-	-	50.
B-1	-	50.	-	1.	49.
B-2	-	50.	-	-	50.
C-1	-	-	50.	1.	49.
C-2	-	-	50.	-	50.
D-1	50.	-	-	1.	49.
D-2	50.	-	-	-	50.

* Composition of Cr spike solution: $K_2Cr(VI)O_4$ (25 mg/L as Cr in experiments A and B, and 18 mg/L as Cr in experiments C and D) added to $CaCO_3$ saturated double-deionized water.

Table 2. Compositions of reactive materials used in dynamic column experiments.

Column	Reactive Mixture Compositions (mass %)		
	Layer 1*	Layer 2	Layer 3
1	99 % quartz sand, 1% calcite (15 cm)		
2	99 % quartz sand, 1% calcite (5 cm)	5% siderite, 95% Layer 1 mixture (5 cm)	99% quartz sand, 1% calcite (5 cm)
3	99% quartz sand, 1% calcite (5 cm)	20% pyrite, 80% quartz sand (10 cm)	95% quartz sand, 5% calcite (5 cm)
4	10% iron chips, 90% quartz sand (10 cm)	+ 1% calcite added to Layer 1 mix (5 cm)	
5	50% iron filings, 50% quartz sand (10 cm)	+ 1% calcite added to Layer 1 mix (5 cm)	
6	50% iron filings, 50% quartz sand (10 cm)	+ 1% calcite added to Layer 1 mix (5 cm)	

* Layer numbering increases upward from base of column

Table 3. Electron-microprobe analyses of fresh and reacted iron chips.

		Fresh Chip		Veinlet, Figure 4b			Figure 5			
				Spot 1	Spot 2	Spot 3	Spot 1	Spot 2	Spot 3	Spot 4
wt%	Fe	99.8	Fe_2O_3	57.5	59.9	99.8	57.9	80.2	54.2	88.4
	Cr	0.0	Cr_2O_3	19.1	20.0	0.4	20.2	3.8	19.9	2.3
	Mn	0.0	CaO	3.8	3.9	0.3	4.1	1.0	4.2	0.6
	Ca	0.0	SiO_2	3.4	1.9	0.4	0.4	3.2	8.6	1.7
	Si	0.0								
	P	0.0								
	sum	99.8		83.8	85.7	100.7	82.6	88.2	86.9	93.0
$(Fe_2O_3 + Cr_2O_3)$/sum				91.4	93.2	99.5	94.6	95.2	85.3	97.5

Table 4. Electron-microprobe analyses of the seven areas of the iron filings marked on Figure 6.

		Area Number, Figure 6						
		1	2	3	4	5	6	7
wt%	Fe_2O_3	51.6	77.4	54.9	56.2	96.7	96.4	96.7
	Cr_2O_3	13.3	4.2	15.3	17.9	0.1*	0.0	0.0
	CaO	3.1	0.8	3.9	4.5	0.0	0.0	0.0
	SiO_2	10.7	1.9	11.1	9.0	1.5	1.5	1.7
	sum	78.7	83.3	85.2	87.6	98.3	97.9	98.4

*Cr present, but at the limit of detection

Table 5. Electron-microprobe analyses for iron filings shown in Figure 8.

		Figure 8						
		Whiter zones				Darker phase		
		1	2	3	4	1	2	3
wt%	Fe	95.9	95.4	95.1	94.3	92.3	90.3	90.7
	Cr	0.3	0.3	0.2	0.3	0.9	0.8	0.9
	P	0.1	0.1	0.0	0.1	0.3	0.7	0.0
	Si	1.9	1.9	2.1	1.8	0.2	0.6	0.0
	Sum*	98.2	97.7	97.4	96.5	93.7	92.4	91.6

*Also present are traces of Ni, Mn, and S. Low totals indicate a missing element, perhaps carbon, or incomplete analysis due to surface irregularities.

Table 6. Concentrations of dissolved constituents (mg/L) in the effluent and calculated saturation indices for the column containing iron filings (column 5).

	Sample	
	193	195
DISSOLVED CONSTITUENT		
Na	3.2	0.2
K	13.8	13.9
Mg	<0.1	<0.1
Ca	4.10	4.60
Fe	<0.02	<0.02
Cu	<0.01	<0.01
Zn	0.23	0.22
Cr	<2	10.
Mn	<0.01	<0.01
Cl	0.6	1.5
SO_4	<2	<2
Reactive Silica	0.8	0.5
pH	9.88	9.77
Eh	229	401
Alkalinity (as $CaCO_3$)	33	33
SATURATION INDICES		
Calcite	0.4	0.4
Amorphous Silica	-2.45	-2.61
$Cr(OH)_3$	0.36	1.08
Ferrihydrite	0.31	0.41
Goethite	6.20	6.30
Lepidocrocite	3.83	3.93
Siderite	-8.79	-11.32

* Calculations were made assuming aqueous concentrations are equal to analytical detection limits.

List of Figures

m/a. Input Cr(VI) concentration was 80 mg/L. a) Cl and b) Cr relative concentrations.

Figure 10. Results of dynamic column experiment for column containing 5 mass% siderite. Average linear velocity of the water through the column was 20 m/a. Input Cr(VI) concentration was 80 mg/L. a) Cl and b) Cr relative concentrations.

Figure 11. Results of dynamic column experiment for column containing 20 mass% pyrite. Average linear velocity of the water through the column was 20 m/a. Input Cr(VI) concentration was 18 mg/L. a) Cl and b) Cr relative concentrations.

Figure 12. Results of dynamic column experiment for column containing 10 mass% iron chips. Average linear velocity of the water through the column was 10 m/a. Input Cr(VI) concentration was 18 mg/L. a) Cl and b) Cr relative concentrations.

Figure 13. Results of dynamic column experiment for column containing 50 mass% iron filings. Average linear velocity of the water through the column was 10 m/a. Input Cr(VI) concentration was 18 mg/L. a) Cl and b) Cr relative concentrations.

Figure 14. Results of dynamic column experiment for column containing 50 mass% iron filings. Average linear velocity of water through the column was 40 m/a. Input Cr(VI) concentration was 18 mg/L. a) Cl and b) Cr relative concentrations.

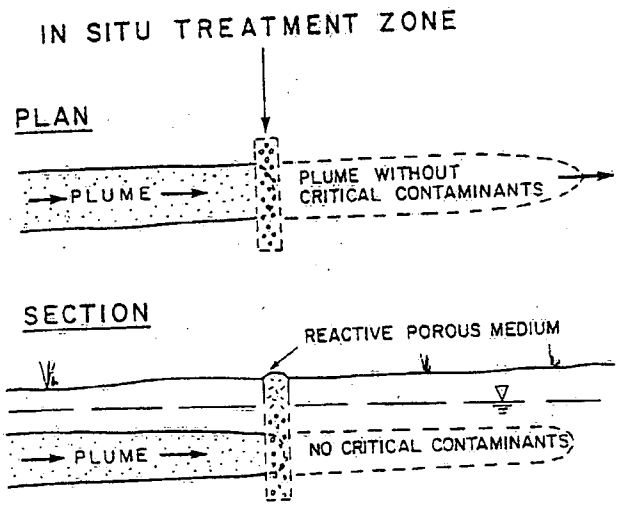

Figure 1
Blowes et al.

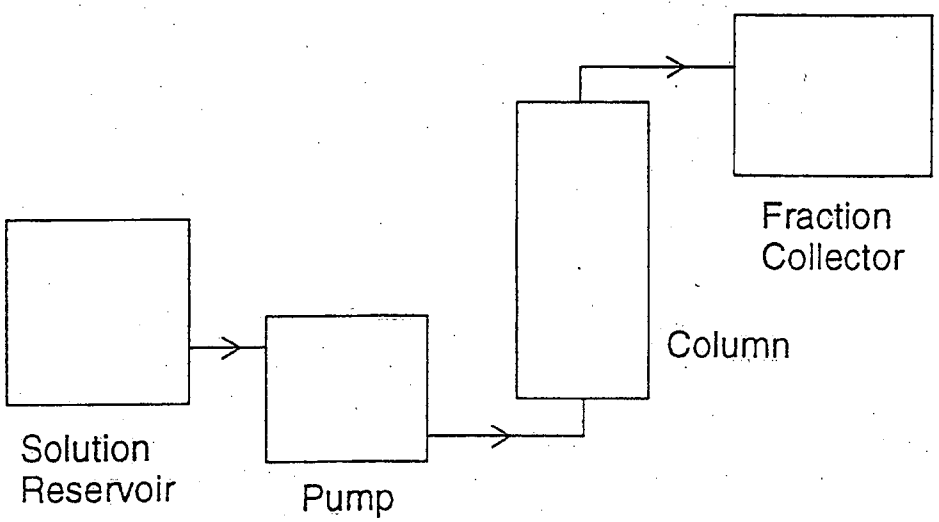

Figure 2
Blowes et al.

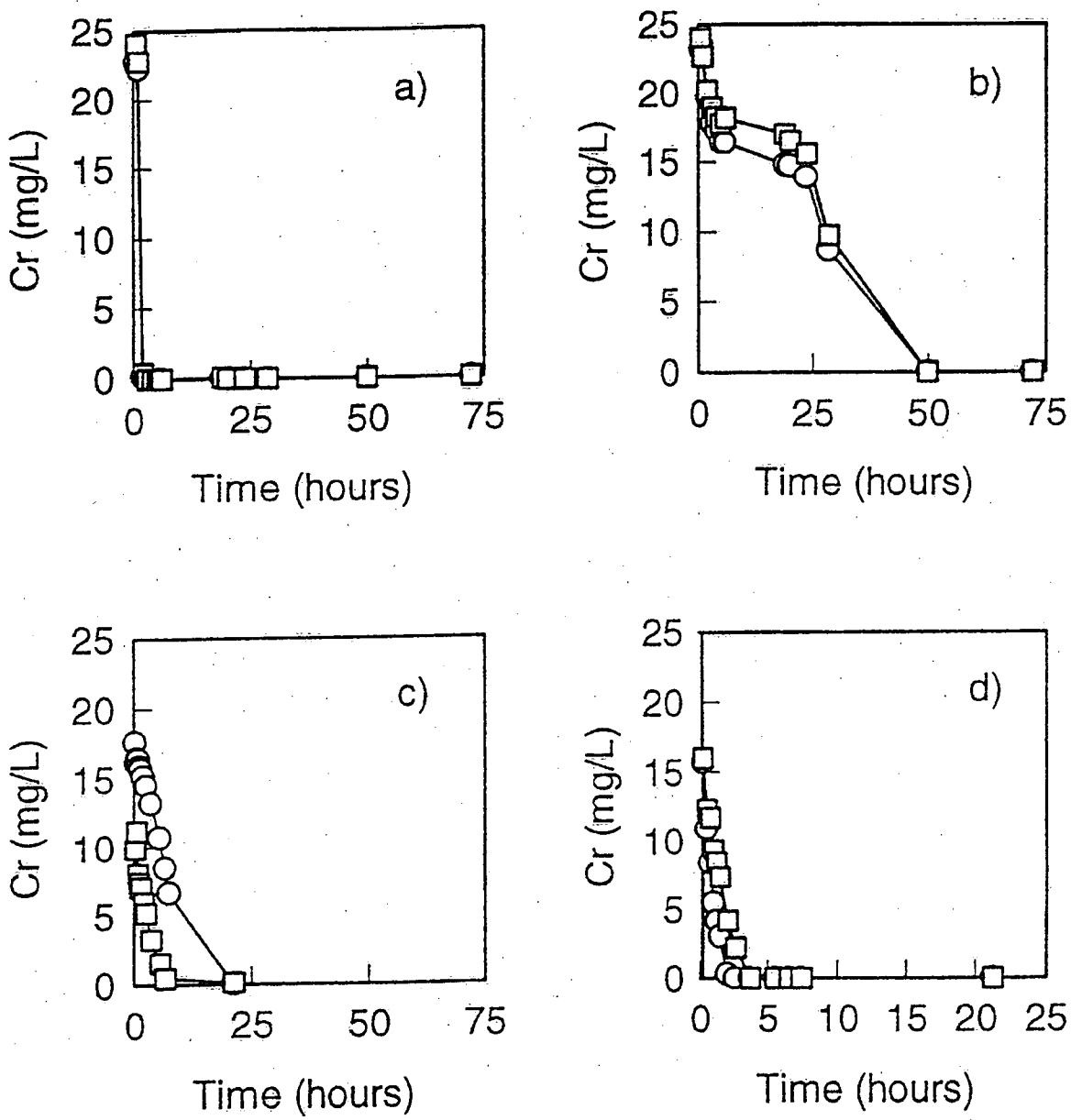

Figure 3
Blowes et al.

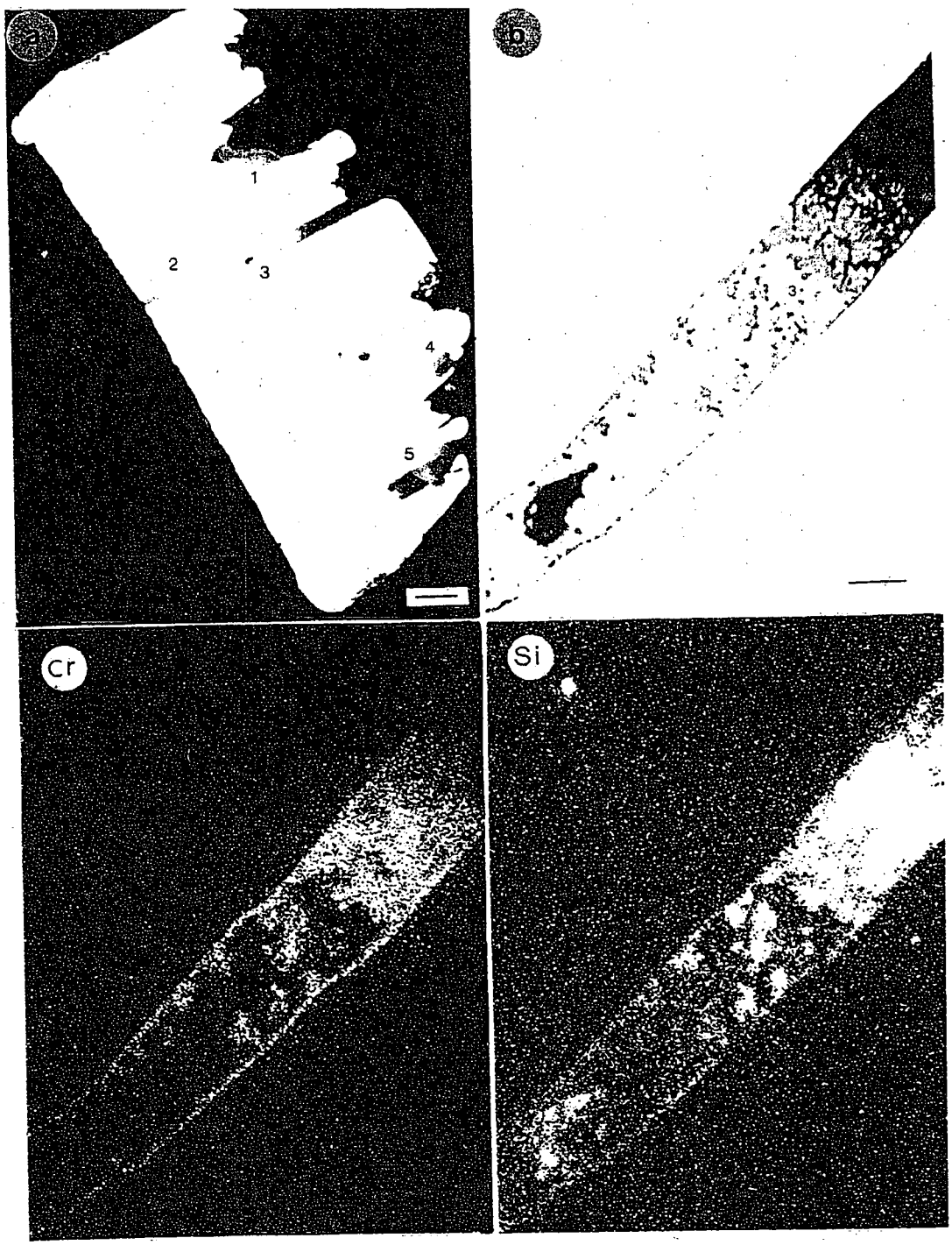

Figure 4.
Blouet et al.

Figure 5 Blowes et al.

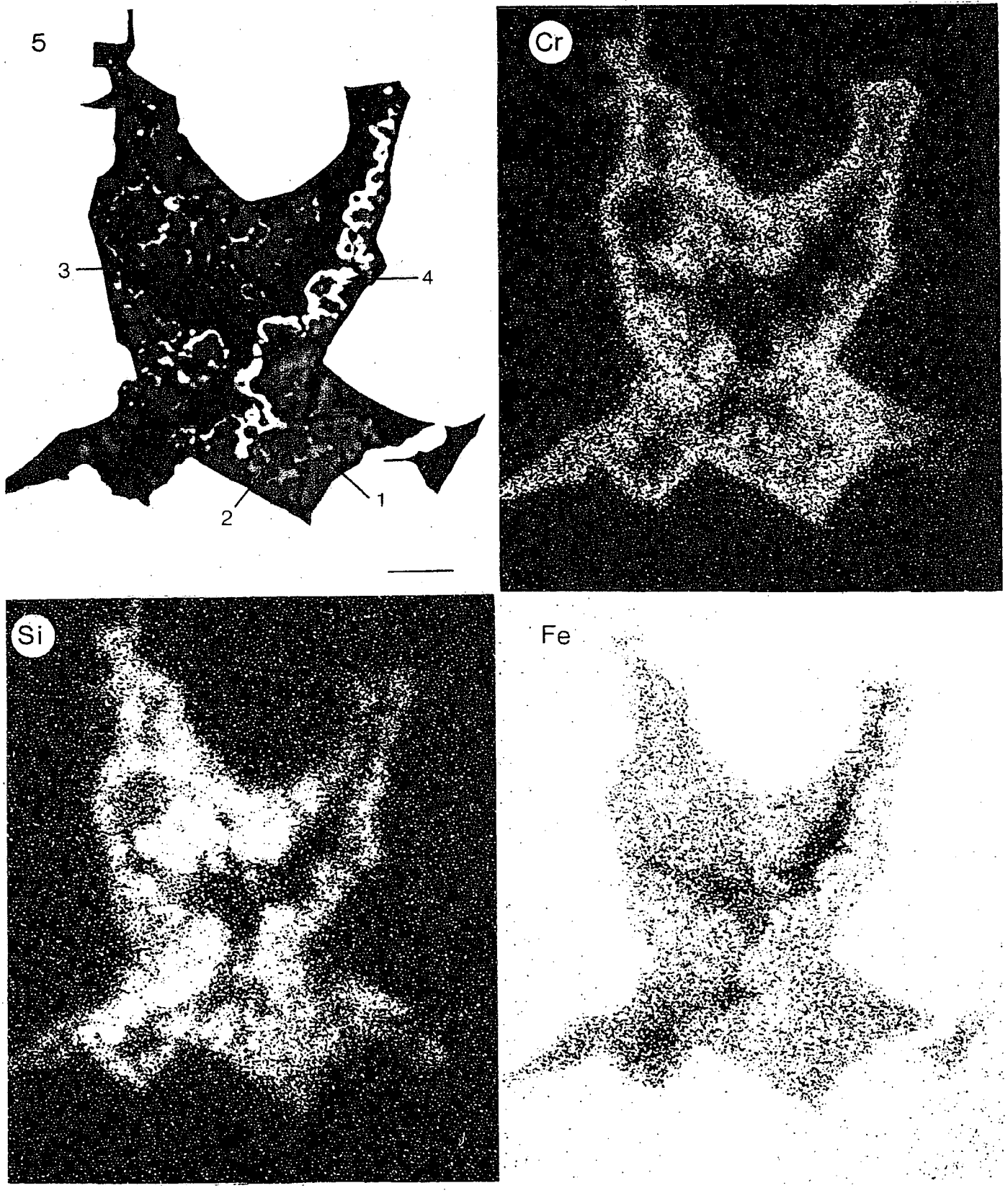

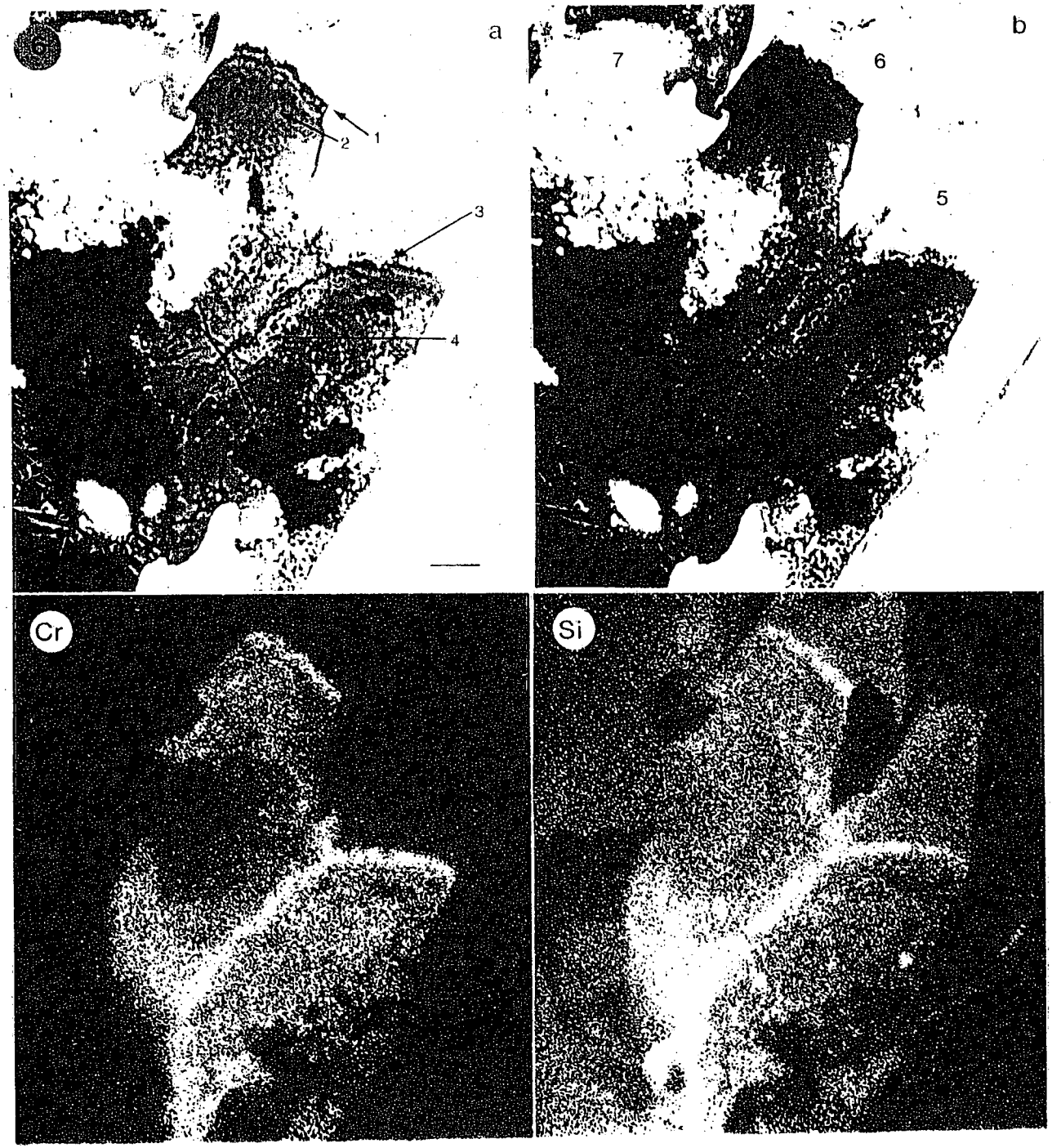
a
b
1
2
3
4
5
6
7
Cr
Si

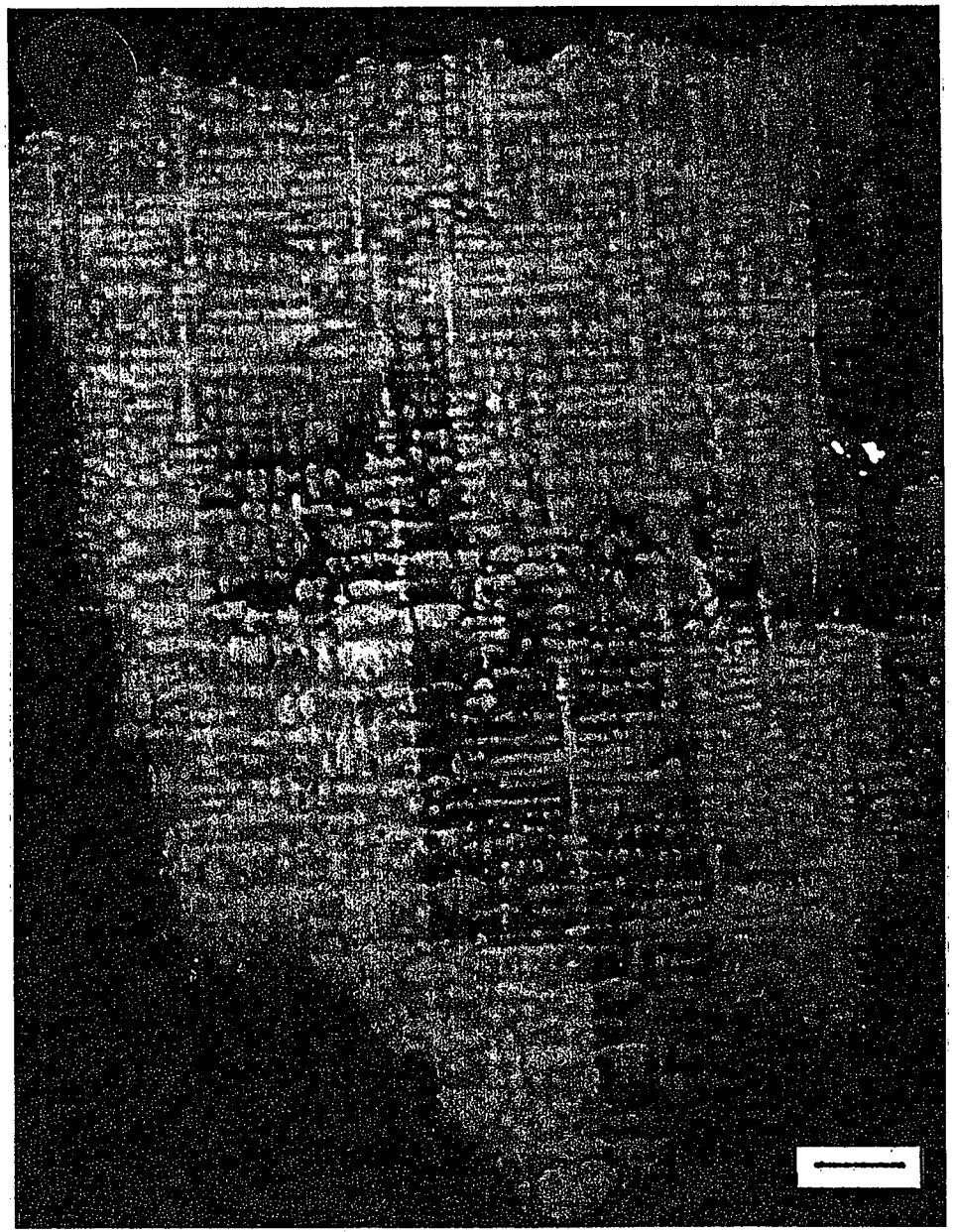

Figure 7.
Blowes et al.

Figure 8 Blowes et al.

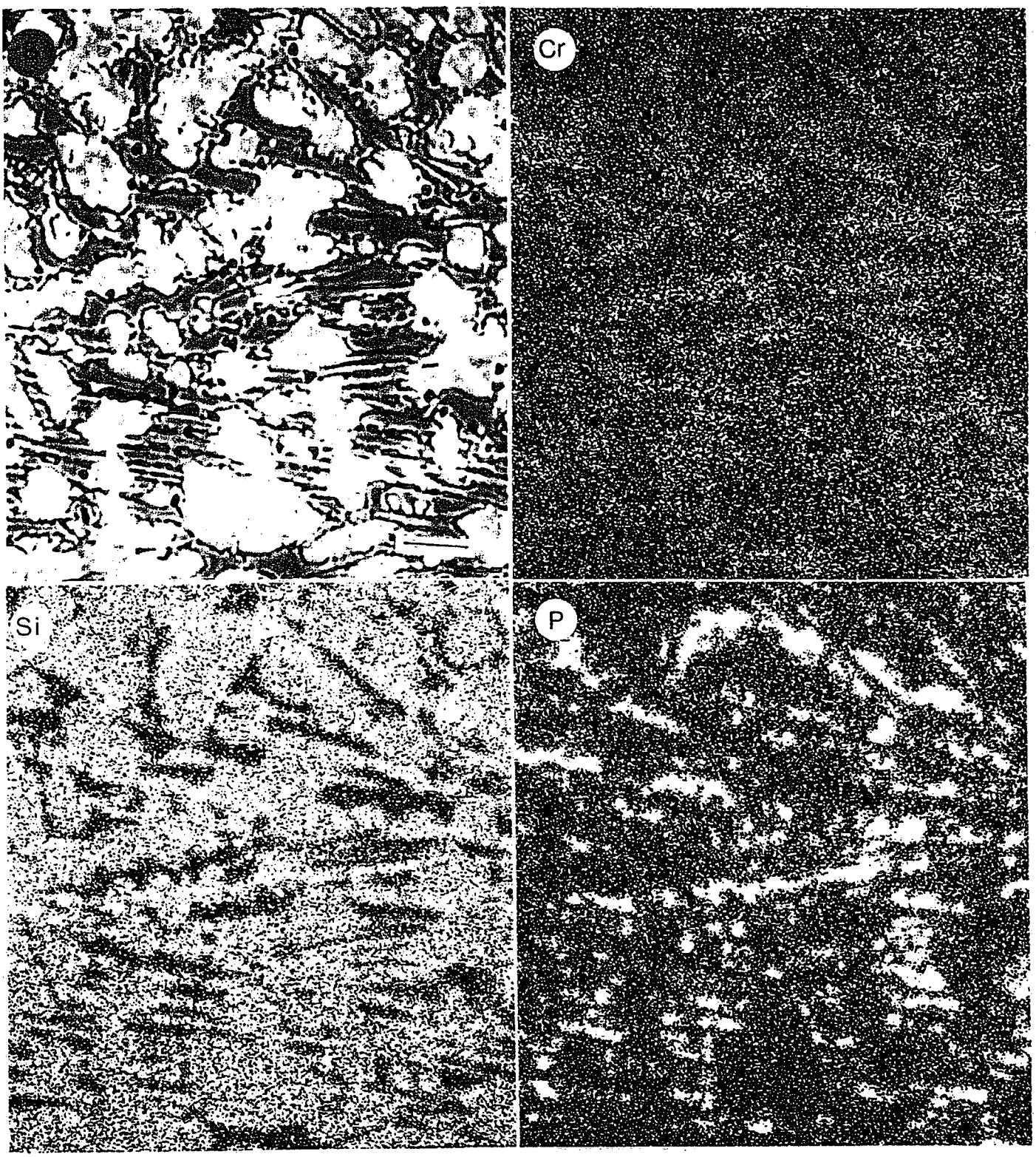

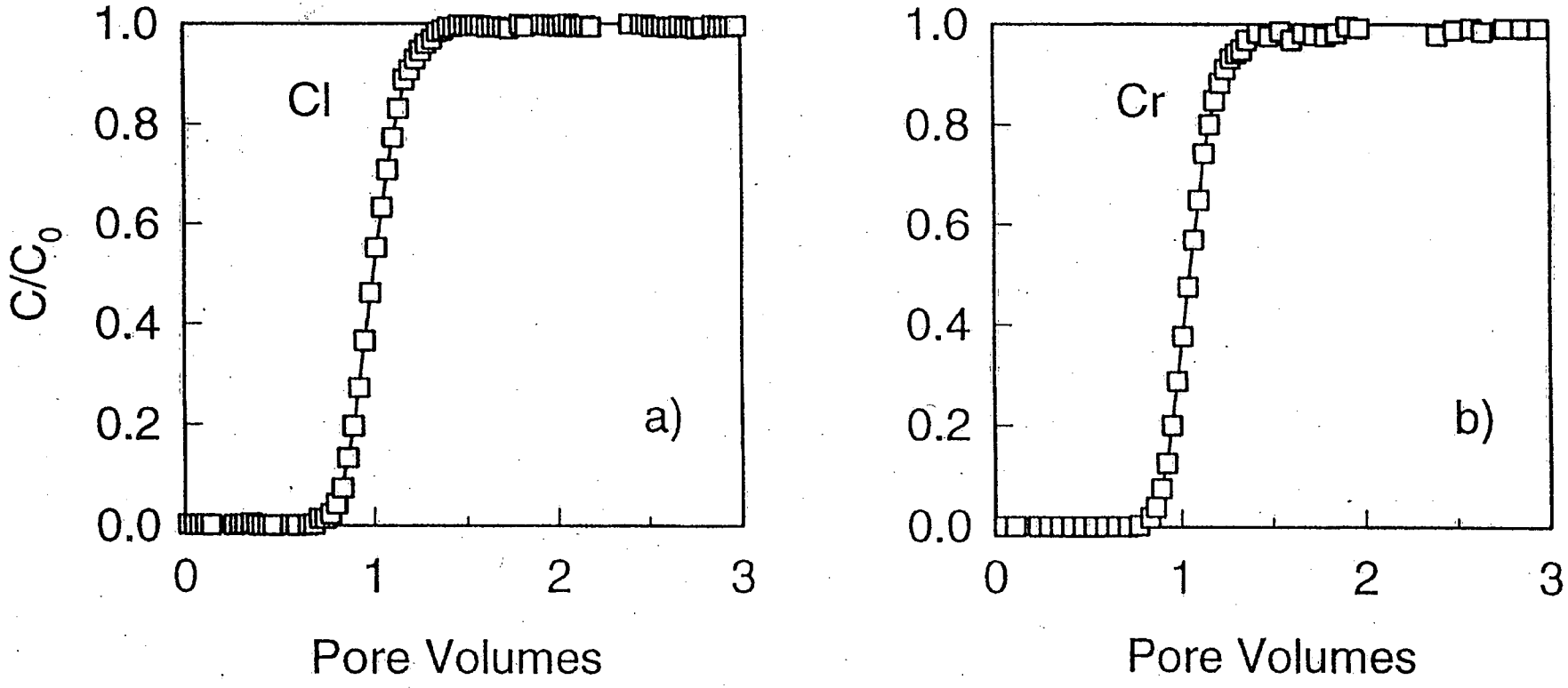

Figure 9
Blowes et al.

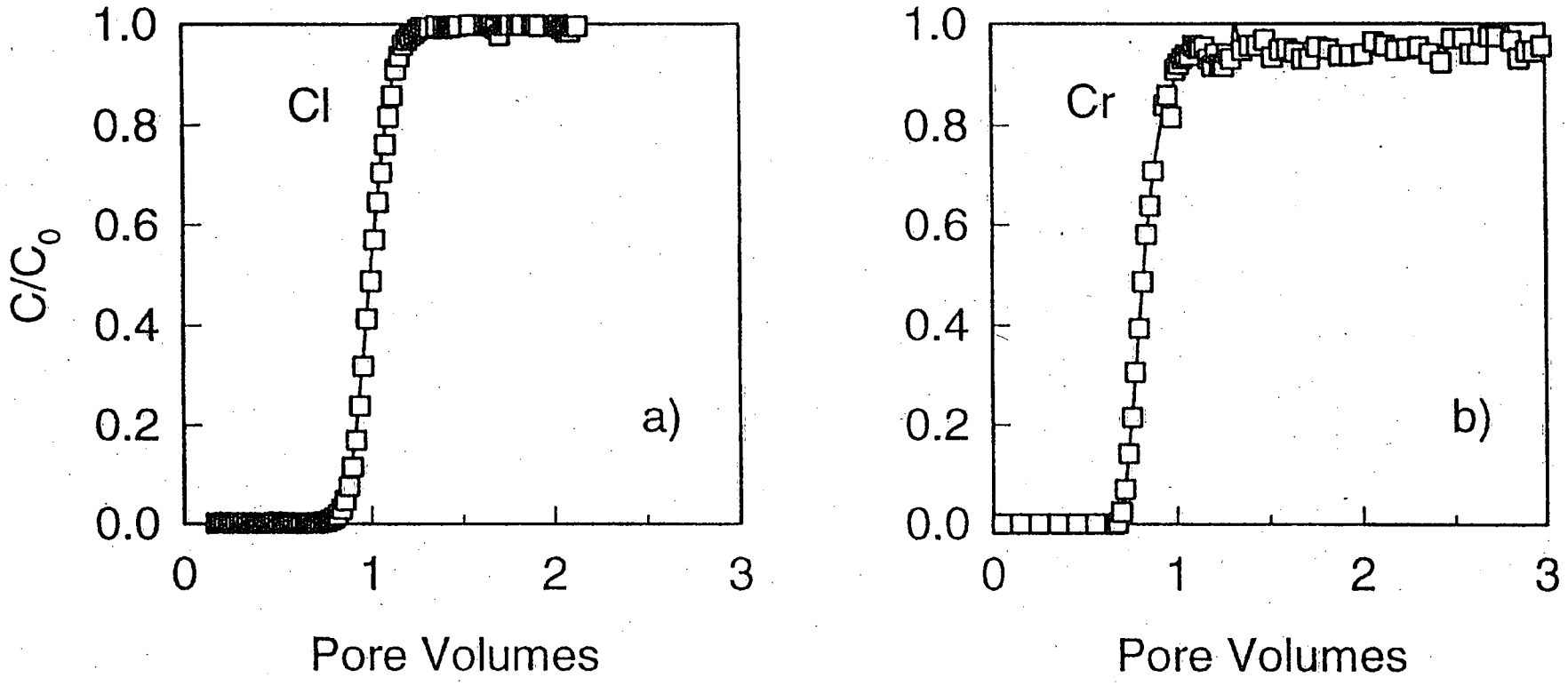

Figure 10
Blowes et al.

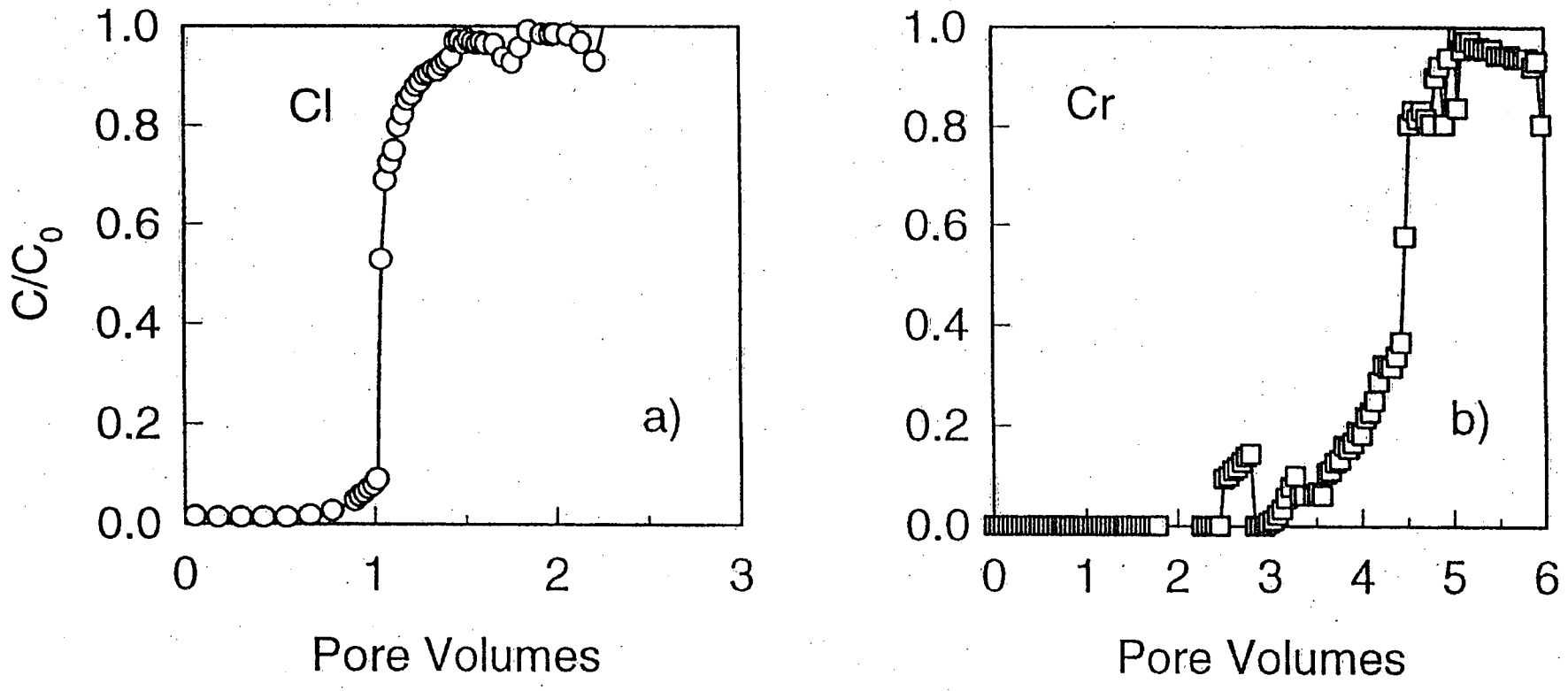

Figure 11
Blowes et al.

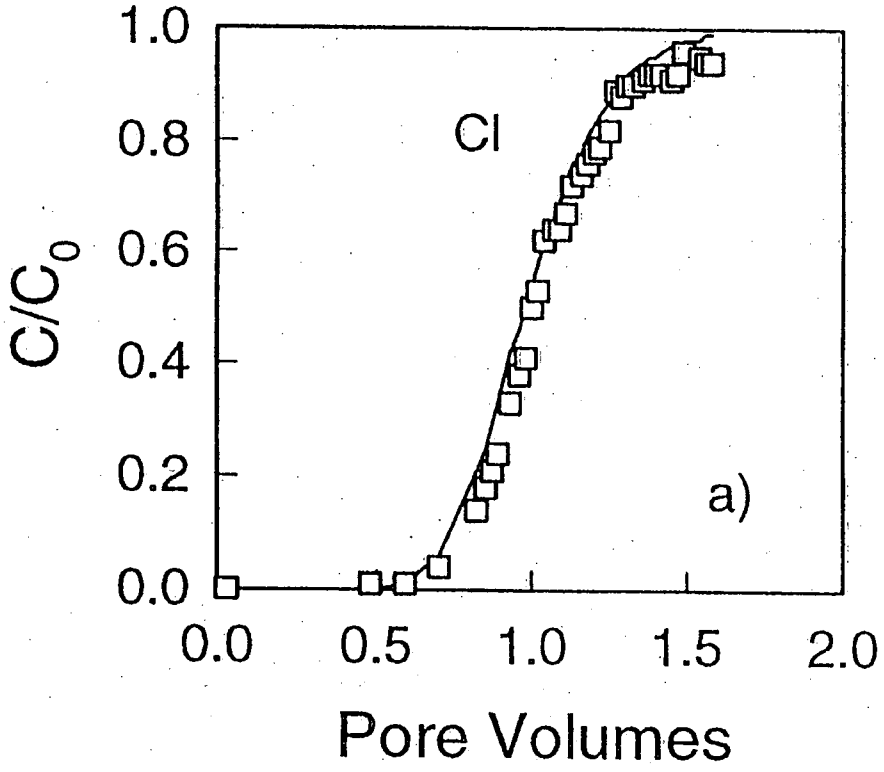

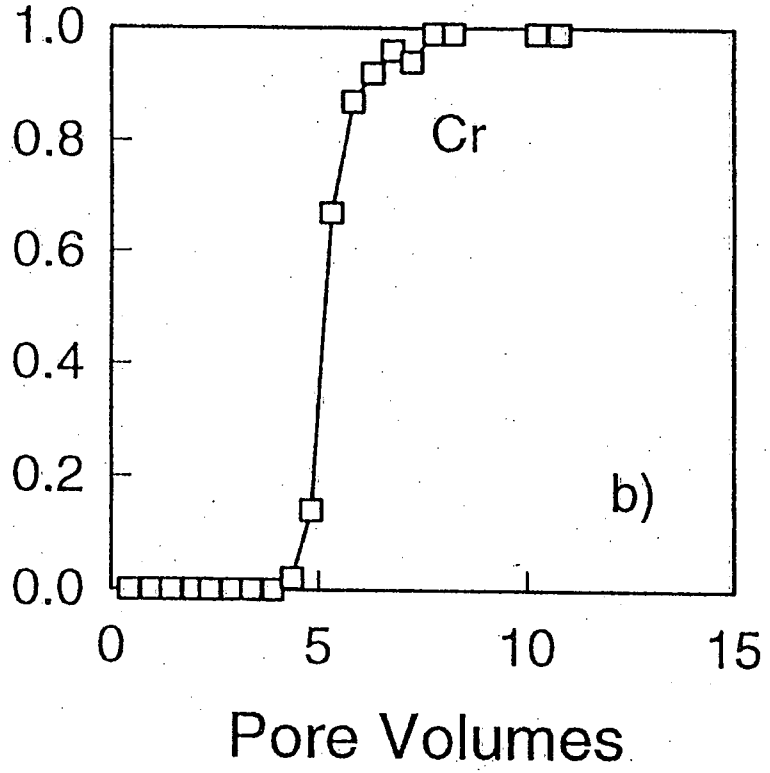

Figure 12
Browes et al.

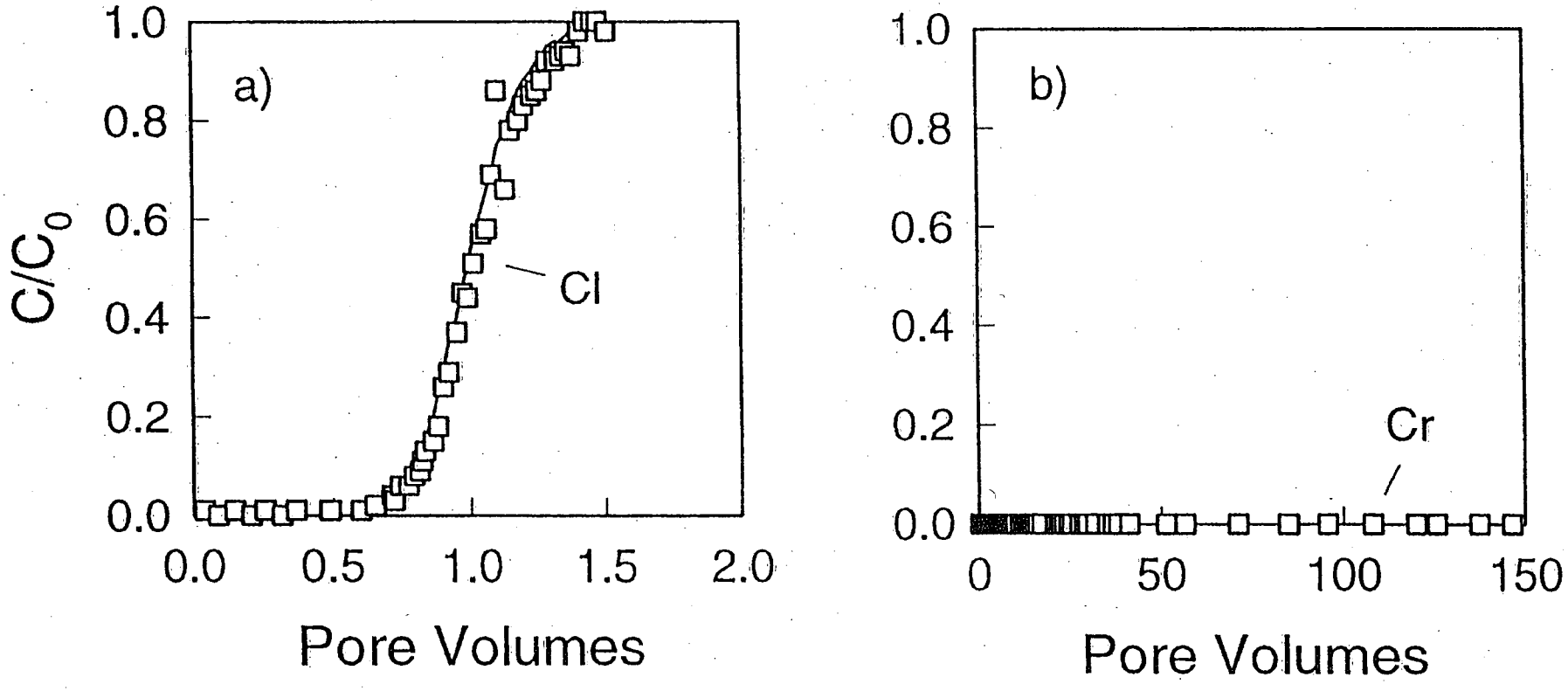

Figure 13
Blowes et al.

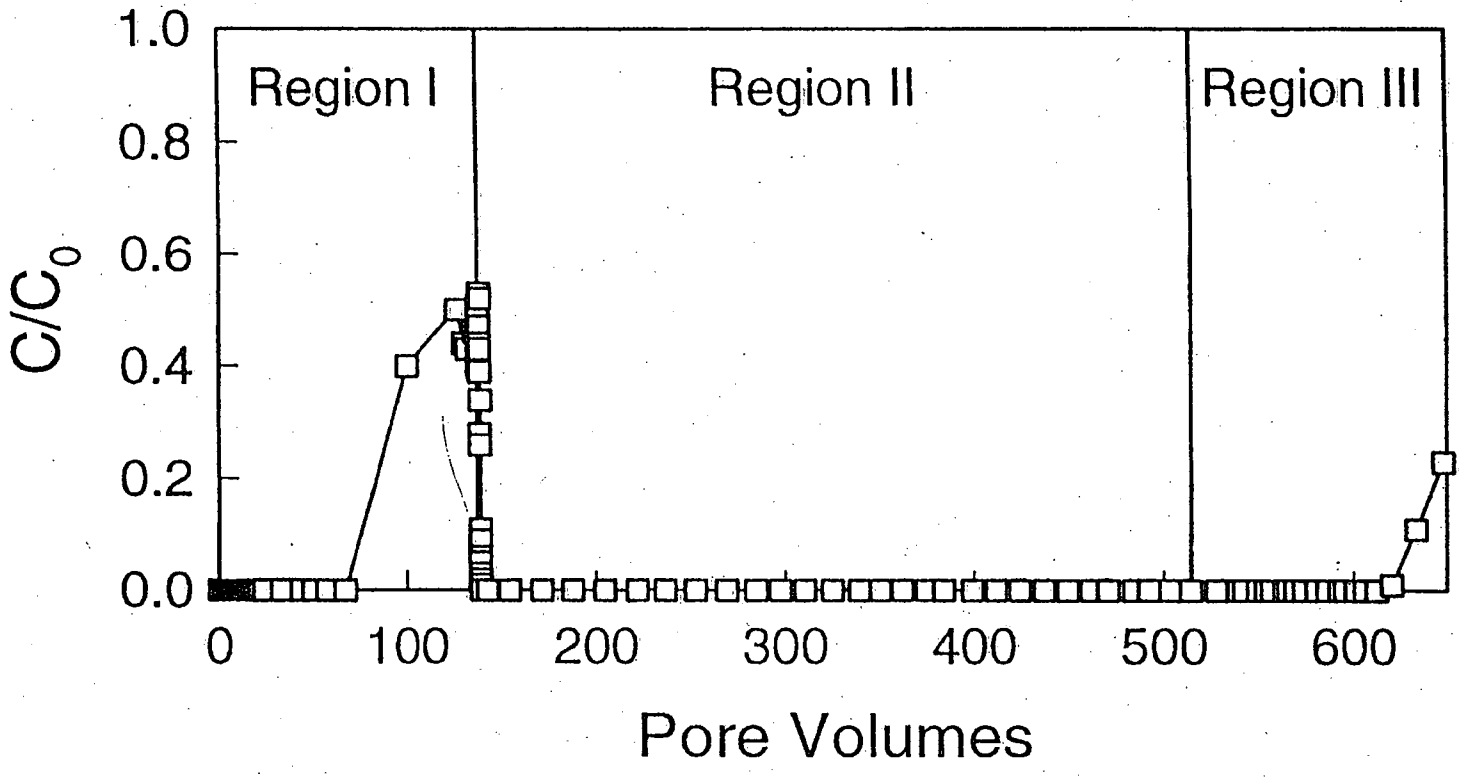

Figure 14
Blowes et al.

Environment Canada Library, Burlington
3 9055 1018 1640 2

Canada Centre for Inland Waters
P.O. Box 5050
867 Lakeshore Road
Burlington, Ontario
L7R 4A6 Canada

National Hydrology Research Centre
11 Innovation Boulevard
Saskatoon, Saskatchewan
S7N 3H5 Canada

St. Lawrence Centre
105 McGill Street
Montreal, Quebec
H2Y 2E7 Canada

Place Vincent Massey
351 St. Joseph Boulevard
Gatineau, Quebec
K1A 0H3 Canada

Centre canadien des eaux intérieures
Case postale 5050
867, chemin Lakeshore
Burlington (Ontario)
L7R 4A6 Canada

Centre national de recherche en hydrologie
11, boul. Innovation
Saskatoon (Saskatchewan)
S7N 3H5 Canada

Centre Saint-Laurent
105, rue McGill
Montréal (Québec)
H2Y 2E7 Canada

Place Vincent-Massey
351 boul. St-Joseph
Gatineau (Québec)
K1A 0H3 Canada